

Feedback of a small-scale magnetic dynamo

S. V. Nazarenko,¹ G. E. Falkovich,² and S. Galtier¹

¹*Mathematics Institute, University of Warwick, Coventry CV4 7AL, United Kingdom*

²*Physics of Complex Systems, Weizmann Institute of Science, Rehovot 76100, Israel*

(Received 6 August 2000; published 21 December 2000)

We develop a WKB approach to the rapid distortion theory for magnetohydrodynamic turbulence with large magnetic Prandtl number. Within this theory, we study the growth of small-scale magnetic fluctuations in a large-scale velocity field being initially a pure strain. We show that the magnetic Lorentz force excites a secondary flow in the form of counterrotating vortices on the periphery of the magnetic spot. Those vortices slow down stretching of the magnetic spot and thus provide a negative feedback for a small-scale magnetic dynamo.

DOI: 10.1103/PhysRevE.63.016408

PACS number(s): 95.30.Qd, 47.27.Gs, 47.27.Jv

I. INTRODUCTION

Probably, the main controversy in the present-day dynamo theory (see [1,2] for a review on the dynamo theory) is related to the role of small-scale magnetic fluctuations. Those are the fastest-growing fluctuations that may change field-generating flow well before the large-scale magnetic field has any chance to grow [3]. This is particularly important when the magnetic Prandtl number (viscosity-to-diffusivity ratio) is high as it seems to be the case for the galactic magnetic field [4]. The kinematic stage of the small-scale magnetic dynamo is well-understood by now [4–7]. The spectrum of magnetic fluctuations grows in amplitude while propagating towards small scales [4]. Whether at the time of feedback appearance this propagation is checked by diffusivity (due to resistivity) or not, the most important conclusion from the kinematic theory is that the maximum of magnetic energy is at the smallest scales available. Certainly, it is a long way from such a spectrum to the steady magnetohydrodynamic (MHD) turbulence which always has the maximum of magnetic energy at large scales.

After the kinematic stage, the next step on this way (called the nonlinear dynamo regime) is to consider a feedback of the small-scale magnetic fluctuations on the large-scale velocity field. This nonlinear problem is difficult to tackle and much less is known about the transition to a saturation phase. One may investigate nonlinear dynamo by direct numerical simulations (DNS) of MHD equations in which the velocity field is now no longer prescribed like in the kinematic case [8–11]. A standard ABC forcing of the velocity field (named after Arnold, Beltrami, and Childress) has been generally used in numerical simulations (see [12] for a forced Taylor-Green vortex). Evidence of the existence of a saturation phase has been shown for different magnetic Prandtl numbers (e.g., up to ~ 10 in Ref. [11]) and a quasi-equipartition between the kinetic and the magnetic energy has often been observed [8–11]. Finally, the effect of magnetic turbulence on the velocity field chaotic properties has also been studied numerically [13,10]. However DNS study is limited to low Reynolds and magnetic Reynolds numbers, and not very high magnetic Prandtl number, due to the 3-D nature of the problem. Therefore, to study the transition from the kinematic to the dynamic regime, one often has to resort

to simplified nonlinear dynamo models [14].

On the other hand a statistical theory of the nonlinear dynamo is expected to be a hard task because of the strong intermittency of dynamo-grown field. Dynamo-generated magnetic fluctuations are intermittent [15] and are localized in spots that occupy a small fraction of the volume. In such cases, a qualitative understanding of particular events and configurations is usually of a great help. Here we develop an analytic formalism to describe the interaction of a large-scale flow and small-scale spectrum of magnetic fluctuation. We take advantage of high magnetic Prandtl number, which (although hard for DNS) simplifies the analytical treatment. We then apply our formalism to describe evolution of a spot of small-scale magnetic fluctuations in the flow that is initially a pure large-scales strain. Numerical simulations are also performed to investigate further this problem. Initially, the spot is axially symmetric and applies no force to the flow. The strain flow breaks the symmetry of the spot, stretching it in one direction and contracting in another. The energy of the magnetic field grows exponentially at the kinematic stage when the back-reaction on the flow is negligible. We show that the secondary flow produced by the back-reaction of the evolving spot is a set of four vortices each centered at the periphery of the spot. Those vortices suppress stretching inside the magnetic spot while accelerate it outside. The result is a negative feedback and the saturation of small-scale dynamo. This seems to agree well with the direct numerical simulations of the feedback of turbulent magnetic dynamo (Cowley and Maron, private communication).

One point has to be specially emphasised about the motivation of the present study. Namely the growth of the magnetic energy can only come at expense of the kinetic energy depletion so that the negative feedback seems to be obvious. Why bother to study it? To answer this question we note that the total energy is not conserved in our system because the velocity fields are not sufficiently localized in space, as will be explained in Sec. III C. In other words, the magnetic spot feedback could initiate an influx of the kinetic energy from infinity which, in principle, could reverse the feedback from negative to positive. Our study shows that an energy influx is indeed present in the system which is seen, for example, in the observed growth of the total energy (even though our

system is dissipative!). However, we will see that such an energy influx does not prevent the dynamo saturation.

II. DERIVATION OF THE GOVERNING EQUATIONS

A. General description

The viscous incompressible MHD equations read

$$(\partial_t + \mathbf{u} \cdot \nabla) \mathbf{u} = -\nabla P_* + \mathbf{b} \cdot \nabla \mathbf{b} + \nu \nabla^2 \mathbf{u}, \quad (1)$$

$$(\partial_t + \mathbf{u} \cdot \nabla) \mathbf{b} = \mathbf{b} \cdot \nabla \mathbf{u} + \sigma \nabla^2 \mathbf{b}, \quad (2)$$

$$\nabla \cdot \mathbf{u} = 0, \quad (3)$$

$$\nabla \cdot \mathbf{b} = 0, \quad (4)$$

where \mathbf{u} is the velocity, \mathbf{b} the Alfvén velocity ($\mathbf{b} = \mathbf{B}/\sqrt{\mu_0 \rho_0}$, with \mathbf{B} the magnetic field, μ_0 the magnetic permeability and ρ_0 the uniform density), P_* the total pressure, ν the kinematic viscosity and σ the magnetic diffusivity. Applying the curl operator to Eq. (1) we obtain the vorticity equation

$$\partial_t \omega_i + u_j \partial_j \omega_i - \omega_j \partial_j u_i = \epsilon_{imn} \partial_{jm} b_j b_n + \nu \nabla^2 \omega_i, \quad (5)$$

where $\omega_i = \epsilon_{ijk} \partial_j u_k$ and ϵ_{ijk} is the antisymmetric tensor. We assume the size of the magnetic spot (and of the secondary flow it produces) to be much larger than the inverse typical wavenumber of magnetic fluctuations. To average over the small-scale magnetic field we apply a WKB formalism based on the Gabor transform [18,19]. In this formalism the average is defined as a space coordinate filter

$$\bar{\boldsymbol{\omega}}(\mathbf{x}, t) = \int \epsilon f^2(\epsilon |\mathbf{x} - \mathbf{x}_0|) \boldsymbol{\omega}(\mathbf{x}_0, t) d\mathbf{x}_0, \quad (6)$$

where f is a function rapidly decreasing at infinity [e.g., $\exp(-x^2)$] such that

$$\int f^2(\mathbf{x}) d\mathbf{x} = 1, \quad (7)$$

and with $\ell/L \ll \epsilon \ll 1$, where ℓ and L are the characteristic lengthscale of magnetic turbulence and the turbulent spot size. The assumption of a large-scale velocity field (i.e., $\bar{\mathbf{u}} = \mathbf{u}$) implies that the vorticity is also a field at large-scale, i.e., $\bar{\boldsymbol{\omega}} = \boldsymbol{\omega}$. Therefore average equation (5) becomes

$$\partial_t \omega_i + u_j \partial_j \omega_i - \omega_j \partial_j u_i = \epsilon_{imn} \partial_{jm} A_{jn} + \nu \nabla^2 \omega_i, \quad (8)$$

with

$$A_{jn}(\mathbf{x}, t) = \overline{b_j b_n} = \frac{1}{(2\pi)^3} \int \hat{b}_j(\mathbf{x}, \mathbf{k}, t) \hat{b}_n(\mathbf{x}, -\mathbf{k}, t) d\mathbf{k}, \quad (9)$$

and where the Gabor transform $\hat{\mathbf{b}}(\mathbf{x}, \mathbf{k}, t)$ of the Alfvén velocity is defined as

$$\hat{\mathbf{b}}(\mathbf{x}, \mathbf{k}, t) = \int f(\epsilon |\mathbf{x} - \mathbf{x}_0|) e^{i\mathbf{k} \cdot (\mathbf{x} - \mathbf{x}_0)} \mathbf{b}(\mathbf{x}_0, t) d\mathbf{x}_0, \quad (10)$$

with the same function $f(x)$ as in Eq. (6). The writing of A_{jn} in terms of Gabor transforms is convenient in this problem as we will see later.

According to the Erthel's theorem we can introduce $\boldsymbol{\eta} = \hat{\mathbf{b}} \mathbf{b}$ and rewrite Eq. (2) as

$$(\partial_t + \mathbf{u} \cdot \nabla) \boldsymbol{\eta} = \sigma \nabla^2 \boldsymbol{\eta}. \quad (11)$$

The Jacobi matrix λ is defined as

$$\lambda_{ij} = \partial_{x_j} a_i, \quad (12)$$

where \mathbf{a} is the initial coordinate of the fluid particles (i.e., $\mathbf{x}(t=0) = \mathbf{a}$). The application of the Gabor transform to Eq. (11) leads to

$$D_t \hat{\boldsymbol{\eta}} = -\sigma k^2 \hat{\boldsymbol{\eta}}, \quad (13)$$

with

$$D_t = \partial_t + \dot{\mathbf{x}} \cdot \nabla + \dot{\mathbf{k}} \cdot \nabla_{\mathbf{k}}, \quad (14)$$

$$\dot{\mathbf{x}} = \mathbf{u}, \quad (15)$$

$$\dot{\mathbf{k}} = -\nabla(\mathbf{k} \cdot \mathbf{u}). \quad (16)$$

The solution of Eq. (11) is readily obtained if we integrate this equation along characteristics (15) and (16). This gives

$$\hat{\boldsymbol{\eta}}(\mathbf{x}, \mathbf{k}, t) = \hat{\mathbf{b}}(\mathbf{a}, \mathbf{q}, 0) e^{q \Gamma \mathbf{q}}, \quad (17)$$

where

$$\Gamma = -\sigma \int_0^t [\lambda \lambda^T]_{\mathbf{x}(\mathbf{a}, t)} dt, \quad (18)$$

$$\mathbf{k} = \lambda^T \mathbf{q}. \quad (19)$$

We now assume that kinematic viscosity (ν) of the fluid is much larger than diffusivity (σ) of the magnetic field, a situation observed for instance in the interstellar medium [16,17] (see also [4]). We shall completely neglect diffusivity in what follows assuming that feedback starts before the smallest scale of magnetic field reaches diffusion scale. As will be seen, feedback stops stretching-contraction evolution of the magnetic spot so no further small scales are produced and our approach is self-consistent. For $\sigma=0$, the Gabor transform of the magnetic field can be written as

$$\hat{b}_j(\mathbf{x}, \mathbf{k}, t) = \lambda_{jl}^{-1}(\mathbf{x}, t) \hat{\boldsymbol{\eta}}_l(\mathbf{x}, \mathbf{k}, t) = \lambda_{jl}^{-1}(\mathbf{x}, t) \hat{\boldsymbol{\eta}}_l(\mathbf{a}, \mathbf{q}, 0). \quad (20)$$

Then we obtain

$$A_{jn} = \lambda_{jl}^{-1}(\mathbf{x}, t) \lambda_{nm}^{-1}(\mathbf{x}, t) \int \hat{b}_l(\mathbf{a}, \mathbf{q}, 0) \hat{b}_m(\mathbf{a}, -\mathbf{q}, 0) \frac{d\mathbf{q}}{(2\pi)^3}. \quad (21)$$

For an isotropic turbulence we write

$$\hat{b}_l(\mathbf{a}, \mathbf{q}, 0) \hat{b}_m(\mathbf{a}, -\mathbf{q}, 0) = \frac{1}{4\pi} \left(\delta_{lm} - \frac{q_l q_m}{q^2} \right) F(\mathbf{a}) Q(|\mathbf{q}|), \quad (22)$$

where functions $F(a)$ and $Q(a)$ determine (arbitrary) initial shape of the turbulent spot and the turbulence spectrum, respectively. It follows that

$$A_{jn} = C \lambda_{jl}^{-1}(\mathbf{x}, t) \lambda_{nl}^{-1}(\mathbf{x}, t) F(\mathbf{a}), \quad (23)$$

where C is a constant defined as

$$C = \frac{1}{4\pi} \int \left(1 - \frac{q_1^2}{q^2} \right) Q(|\mathbf{q}|) \frac{d\mathbf{q}}{(2\pi)^3}. \quad (24)$$

The relation (23) implies that only the intensity of $Q(|\mathbf{q}|)$ is important, not its form. Therefore the constant C appears as the initial intensity of the magnetic turbulence.

B. The Stokes regime

Let us consider now a particular case of the initial velocity field being pure two-dimensional strain $\mathbf{u} = (s_0 x, -s_0 y, 0)$. Not only this is a simple model of a dynamo-generated flow yet also known to be most dynamo-effective when magnetic diffusivity is taken into account [7]. In the case of large magnetic Prandtl number, $\nu \gg \sigma$, a significant amount of magnetic energy is concentrated at the scales smaller than the dissipative scale of the kinetic energy (Kolmogorov scale). Thus we will consider now the Stokes regime where the Reynolds number is small ($L^2 s_0 \ll \nu$). Then for a two-dimensional strain we can rewrite Eq. (8) in the stationary case as the following linear equation

$$(\partial_{11} - \partial_{22}) A_{12} + \partial_{21} (A_{22} - A_{11}) + \nu \nabla^2 \omega_3 - \partial_t \omega_3 = 0. \quad (25)$$

Note that we did not assume smallness of ω_3 with respect to s_0 , so that the secondary flow is allowed to be as strong as the initial strain flow. Note that even though $\partial_t \omega_3$ term is important initially (since $\omega_3 \equiv 0$ at $t=0$) it will soon turn negligible under the condition $\nu \gg s_0 L^2$ where L^2 is the (smaller) dimension of the magnetic spot. We assume this condition to be satisfied initially and then it only improves and the spot contracts in y -direction. We checked numerically that indeed $\partial_t \omega_3$ term is negligible except for a very short initial interval of time (see Fig. 1 and Sec. III A). After neglecting this term, Eq. (25) turns into a Poisson equation so that vorticity could be found analytically for any given spatial form of the magnetic spot. At $t=0$, $A_{12}=0$ while $A_{11}=A_{22}$. The initial evolution then can be studied analytically taking A from a kinematic stage. One can easily convince oneself that as time goes, the main term will be $-\partial_{21} A_{11}$. Then,

$$\omega_3(x, y, t)$$

$$= \nu^{-1} \int \int_{-\infty}^{\infty} \frac{A_{11}(x', y', t)(x-x')(y-y')}{[(x-x')^2 + (y-y')^2]^2} dx' dy'. \quad (26)$$

That shows that vorticity has to appear as four vortices (because of $x \rightarrow -x$ and $y \rightarrow -y$ symmetries) having centers

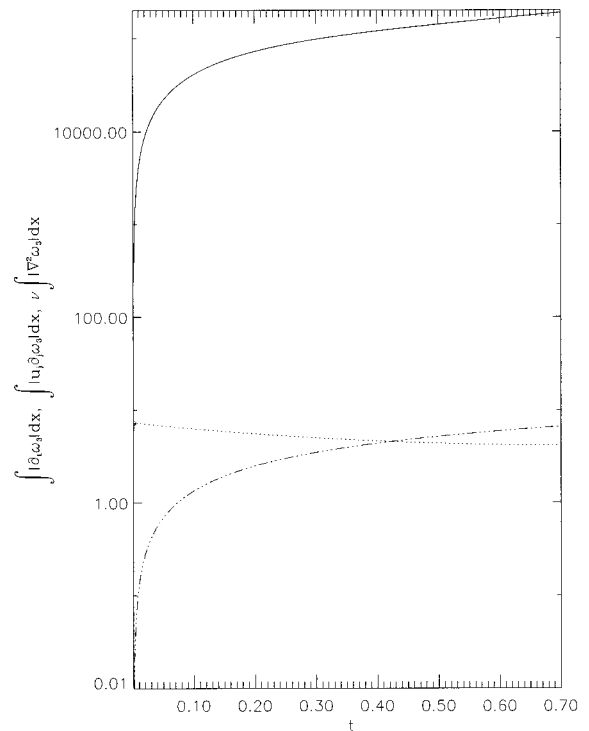


FIG. 1. Temporal evolution in linear-log coordinates of the dissipative term (solid line), inertial terms (dash-dotted line) and time derivative of the vorticity (dotted line) which appear in Eq. (8). The three quantities are integrated in absolute value in the entire box.

where $-\partial_{21} A_{11}$ is maximal (i.e., on the periphery of the spot), the sign of vorticity is negative in the $(x > 0, y > 0)$ domain. To study a later stage when feedback is substantial we have to complete the system (23) and (25) by the following equation

$$D_t \mathbf{a} = (\partial_t + \mathbf{u} \cdot \nabla) \mathbf{a} = 0, \quad (27)$$

which describes the evolution of the initial coordinates of the fluid particles. For that we define the velocity field as

$$\mathbf{u} = (s_0 x + \partial_y \psi, -s_0 y - \partial_x \psi), \quad (28)$$

where s_0 is the strain and ψ is the stream function related to the vorticity ω_3 by the relation

$$\omega_3 = -\nabla^2 \psi. \quad (29)$$

We will consider in our study the initial coordinates

$$\mathbf{a} = (a_x, a_y) = (x, y), \quad (30)$$

with a vorticity ω_3 taken initially null. Then the algorithm to solve the system is the following: using the initial condition (30) we solve Eq. (23) which leads to the value of the vorticity through the resolution of Eq. (25). The value of the stream function is deduced from Eq. (29). Finally we have to solve Eqs. (28) and (27) to come back to the beginning of the loop.

C. Kinematic stage

For the purpose of future comparison let us mention briefly the well-known facts about the evolution during the kinematic stage in the uniform strain flow. It is straightforward to show that the vector \mathbf{a} evolves according to

$$\mathbf{a} = (xe^{-s_0 t}, ye^{+s_0 t}), \quad (31)$$

and therefore the Jacobi matrix is

$$\lambda = \begin{pmatrix} e^{-s_0 t} & 0 & 0 \\ 0 & e^{s_0 t} & 0 \\ 0 & 0 & 1 \end{pmatrix}. \quad (32)$$

This result means that all terms A_{jn} , $j \neq n$, are null. In our numerical simulations (see Sec. III) the function F is defined as

$$F(\mathbf{a}) \propto \exp(-4(a_x^2 + a_y^2)) \quad (33)$$

in order to decrease rapidly at infinity. $F(\mathbf{a})$ can be seen as a measure of the size of the turbulent spot. According to Eq. (31) we see that the magnetic turbulence, initially contained in a disk centered at the origin, will flatten in the y -direction because of its interaction with the uniform strain flow. The description proposed here will become invalid when the size of the spot will reach the size of the strain field, i.e., when the intermediate scale will reach the size of the large scale.

III. NUMERICAL RESULTS

A. Initial setup and accuracy

Let's present now the numerical simulations of the feedback. The temporal evolution of the feedback in the Stokes regime is governed by the system of six equations (30), (23), (25), (29), (28), (27) derived above. The numerical resolution of such a system does not present any particular difficulty except for the Poisson equation (25,29) for which a full multi-grid algorithm is used. All computations have a resolution of 512×512 grid points in a box of size $L_B \times L_B$, with a length $L_B = 8$. The values $s_0 = 1$, $\nu = 2 \times 10^4$ and $C = 4 \times 10^4$ are used. They have been chosen in order to equalize the contribution of the dissipative term to the magnetic term ($\nu \sim A_{11}/s_0$) and to have a small Reynolds number ($A_{11}L^2/\nu^2 \ll 1$). In both cases the magnetic contribution is represented by the dominant term A_{11} which can be substituted for the intensity of the magnetic turbulence C . With this choice of parameters we see that at time of order one the ratio between the kinetic energy and the magnetic energy, $s_0 L^2/\nu$, is much smaller than one. The initial velocity field is a pure two-dimensional strain. The resolution of Eq. (27) leads after a finite time to unavoidable numerical problems. In practice they appear from time $t \sim 0.8$ which will be considered consequently as the final time of computations. Note that our WKB formalism and the symmetry of the flow allowed us to reduce the three-dimensional problem to a two-dimensional one.

In order to prove that we are consistent with the assumption made in Sec. II B about the negligible role played by $\partial_t \omega_3$ (and by the nonlinear terms), we have first performed a simulation including Eq. (8) instead of Eq. (25). The algorithm used to solve Eq. (8) is the following: first we solve the left-hand-side of Eq. (8) and then the value found for ω_3 is used to compute the right-hand side terms. Then at the next step the right-hand side terms are taken into account to correct the Poisson equation constituted by the left-hand side of Eq. (8). The result is displayed in Fig. 1: it is the temporal evolutions of the time derivative of the vorticity $\int |\partial_t \omega_3| d\mathbf{x}$, inertial terms $\int |u_j \partial_j \omega_3| d\mathbf{x}$, and dissipative term $\nu \int |\nabla^2 \omega_3| d\mathbf{x}$. The absolute values are taken to give the order of magnitude of the different quantities. As expected the term $\partial_t \omega_3$ is important only initially, then the dissipative term is greatly dominant. Consequently in the rest of this study we will consider that the resolution of Eq. (25) is good enough to describe the regime that we are dealing with.

B. Negative feedback and saturation

Figure 2 shows the contour plots of $A_{11}(x, y)$ at times $t = 0.005, 0.4, 0.6$, and 0.8 . Hereafter only a quadrant is going to be considered because of the symmetry of the problem. We clearly see on this quadrant the effect of the strain flow on the spot which consists to break the initial symmetry by stretching the spot in one direction and contracting it in another. Note that the spot distortion at the kinematic stage would lead to elliptic contours, and the observed deviation from the elliptic shape is due to the back-reaction of turbulence. This back-reaction is seen in Fig. 3: it is the contour plot of the vorticity $\omega_3(x, y)$ for the same times as in Fig. 2. A negative vortex is produced at the periphery of the spot. Here again the initial symmetry is lost due to the effect of the strain flow.

Temporal evolution of magnetic energy is displayed in Fig. 4: on top we have the evolution of $\int A_{11} d\mathbf{x}$ and $A_{11}(\mathbf{x}_c, 0)$ with $\mathbf{x}_c = (0.15625, 0.15625)$. A comparison is made with the exponential law of index 2 that A_{11} should follow in the kinematic case. For convenience the two quantities are normalized to their initial values. In the first stage, A_{11} follows the exponential law but soon we observe a deviation which amplifies with time. We interpret that as a saturation effect due to the negative feedback of small scales, this saturation being more important closer to the center of the spot. Note that at the final time of the computation the growth of the total energy, which is more or less $\int A_{11} d\mathbf{x}$, is smaller than that obtained without feedback by a factor ~ 1.56 . The bottom of Fig. 4 deals with the temporal evolution of the total energy, the magnetic energies $\int A_{11} d\mathbf{x}$ and $\int A_{22} d\mathbf{x}$. The plots are compared with exponential laws of indices 2 and -2 . Note the symmetrical evolution of the two quantities. Temporal evolution in log-log coordinates of the kinetic energy of the secondary flow integrated in the entire box is given in Fig. 5. As we see, it behaves roughly like a power law of index 2. We note finally that the kinetic energy of the secondary flow is negligible compared to the magnetic energy at all times (see also Fig. 4).

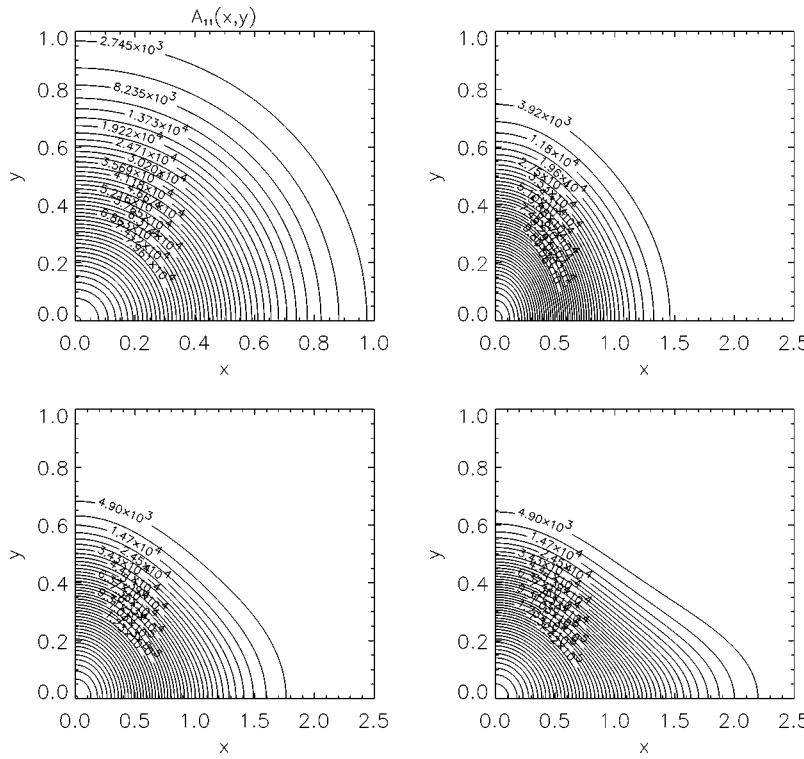


FIG. 2. Contour plots of $A_{11}(x,y)$ at times $t = 0.005, 0.4, 0.6$, and 0.8 . Note the different scaling of the x - and y -axes for the last three times. Only a fraction of the numerical box is shown. A deviation from the elliptic shape is observed.

Figure 6 shows the temporal evolution of the velocity gradient $\partial u(x_j,0)/\partial x$ at different points $(x_j,0)$ along the x -axis such that $x_j = 0, 0.25, 0.5$, and 1.0 . This quantity measures the strain modifications by the secondary flow. Note

that strain reduction at the origin provides the mechanism for the negative feedback and the turbulence saturation. A comparison is made with an exponential law of index -2 . The gradient decreases more strongly closer to the origin,

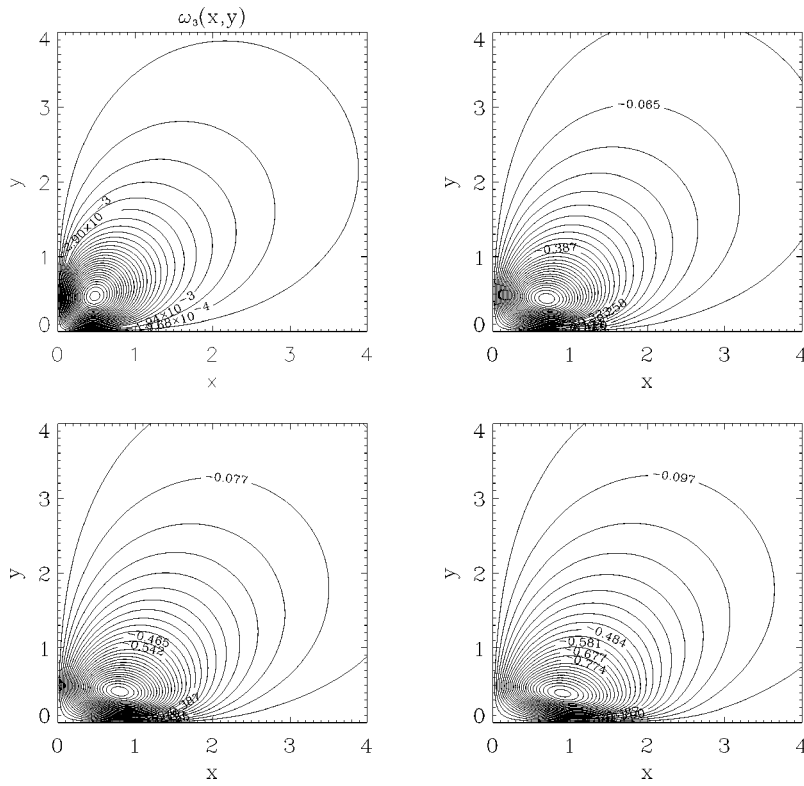


FIG. 3. Contour plots of the vorticity $\omega_3(x,y)$ at times $t = 0.005, 0.4, 0.6$, and 0.8 . Note the negative value of the vorticity; note also that the absolute value of the vorticity increases in time. Only a fraction of the numerical box is shown.

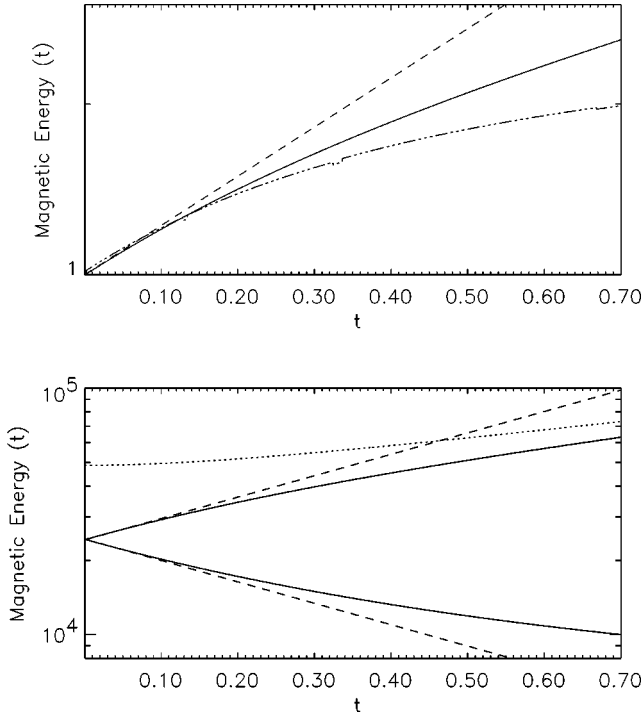


FIG. 4. (Top) Temporal evolution in linear-log coordinates of $\int A_{11} d\mathbf{x}$ (solid line). A comparison is made with $A_{11}(\mathbf{x}_c, 0)$ (dash-dotted line) at the point $\mathbf{x}_c = (0.15625, 0.15625)$ and with an exponential law of index 2 (dashed line). The plots are normalized to initial values [2.4×10^4 for the integrated quantity, and $A_{11}(\mathbf{x}_c, 0) \approx 1.1 \times 10^5$]. (Bottom) Temporal evolution in linear-log coordinates of the total energy (dotted line), magnetic energies $\int A_{11} d\mathbf{x}$ (increasing solid line) and $\int A_{22} d\mathbf{x}$ (decreasing solid line). The plots are compared with exponential laws of indices 2 and -2 (dashed line).

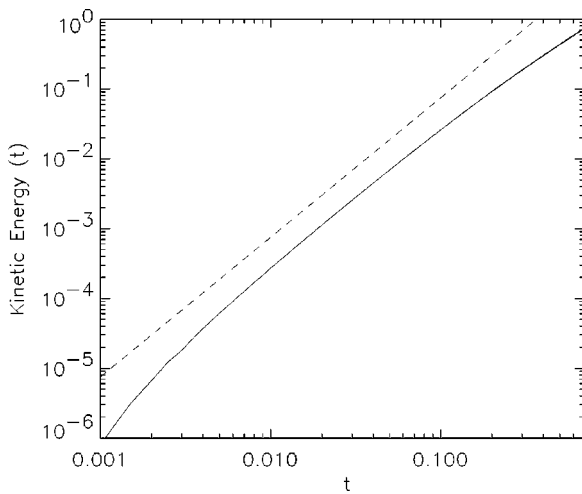


FIG. 5. Temporal evolution in log-log coordinates of the kinetic energy of the secondary flow (solid line) integrated in the entire box. A comparison is made with a power law of index 2 (dashed line). Note that the kinetic energy plays a negligible role in the temporal evolution of the total energy (see also Fig. 4).

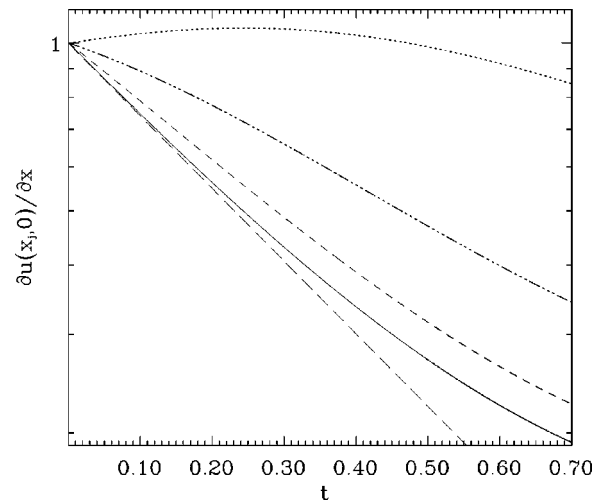


FIG. 6. Temporal evolution in linear-log coordinates of the velocity gradient $\partial u(x_j, 0) / \partial x$ at different points $(x_j, 0)$ located along the x -axis such that $x_j = 0$ (solid line), 0.25 (dashed line), 0.5 (dash-dotted line), and 1.0 (dotted line). A comparison is made with an exponential law of index -2 (long dashed line).

however its value never cross the axis $y=0$. The temporal evolution of integrated vorticity $-\int \omega_3 d\mathbf{x}$ is given in Fig. 7. It follows approximately a power law of index 1.

C. Energy conservation

Figure 8 shows the temporal evolution of the total energy $\int [E_T - E_T(t=0)] d\mathbf{x}$ in which the kinetic energy of the strain flow is not included, changes magnetic energies $\int [A_{11} - A_{11}(t=0)] d\mathbf{x}$, $\int [A_{22}(t=0) - A_{22}] d\mathbf{x}$, components of the kinetic energy $\int (\partial_y \Psi)^2 d\mathbf{x}$, $\int (\partial_x \Psi)^2 d\mathbf{x}$ and dissipated kinetic energy $\nu \int_0^t \int (\omega_3(\mathbf{x}, t'))^2 d\mathbf{x} dt'$. We observe that each quantity increases in time, including the total energy. As we said before, the kinetic energy is defined as the integral of the square velocity of the secondary flow. It is equal to the total kinetic energy minus the kinetic energy of the background strain flow $\frac{1}{2} \int ((\mathbf{U} + \mathbf{u})^2 - \mathbf{U}^2) d\mathbf{x}$, because the cross term

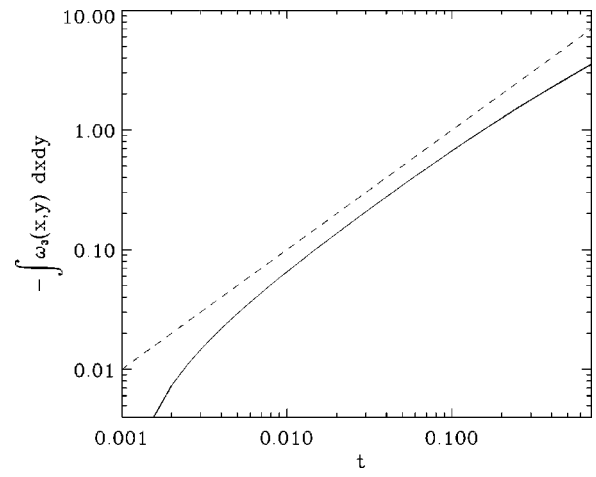


FIG. 7. Temporal evolution in log-log coordinates of the integrated vorticity $-\int \omega_3 d\mathbf{x}$ (solid line). A comparison is made with a power law of index 1 (dashed line).

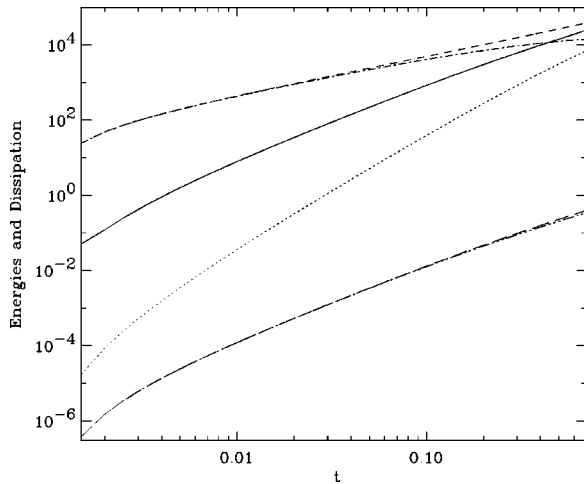


FIG. 8. Temporal evolution in log-log coordinates of the total energy $\int E_T d\mathbf{x} - \int E_T(t=0) d\mathbf{x}$ (solid line), $\int A_{11} d\mathbf{x} - \int A_{11}(t=0) d\mathbf{x}$ (dashed line), $\int A_{22}(t=0) d\mathbf{x} - \int A_{22} d\mathbf{x}$ (dash-dotted line), $\int (\partial_y \Psi)^2 d\mathbf{x}$ (long dashed line), $\int (\partial_x \Psi)^2 d\mathbf{x}$ (dash-three-dotted line), and $\nu \int_0^t \int (\omega_3)^2 d\mathbf{x}$ (dotted line). Note increase of the total energy.

$2\int \mathbf{U} \cdot \mathbf{u} d\mathbf{x}$ equals zero. It may seem strange that the total energy, the sum of the magnetic and kinetic energies, is increasing. Explanation of this fact is in an insufficiently fast decrease at infinity of the velocity field generated by the vortex quadrupole ($u \sim 1/R^3$ where R is the distance from the quadrupole's center). Because of that the integral over the entire space of the energy flux terms like $(\mathbf{n} \cdot \mathbf{U})(\mathbf{U} \cdot \mathbf{u})$ where \mathbf{n} is the normal to the domain of integration (in the local energy equation), diverges and it is not possible to obtain any global energy equation. This situation is similar to the problem without magnetic field where a turbulent spot of high Reynolds number velocity perturbations is placed in an external large-scale strain [18]. In this case, the total energy is also increasing because of the similar reasons. It is interesting that if we had a multipole vortex structure with the number of poles greater than four then its velocity field would decay faster than R^{-3} and the total energy would be conserved.

IV. CONCLUSIONS

In this paper, we have developed a WKB formalism to the rapid distortion theory for MHD turbulence, at large magnetic Prandtl number, in order to study the nonlinear dynamo problem and understand the origin of the saturation phase. The interaction between a spot of small-scale magnetic fluctuations and a flow seen like a pure strain at large scales has been considered. The effect of the strain flow is to break the initial symmetry of the spot by stretching it in one direction and contracting in another. The main property that we have observed is the generation of a set of four vortices along the sides of the spots due to the back-reaction of the evolving spot. The vortices are such that they tend to suppress stretching inside the magnetic spot while accelerate it outside. This effect leads to a negative feedback and provides a saturation mechanism of small-scale dynamo. Even though the initial flow of two-dimensional pure strain has been considered, it is claimed that the results are representative of wide classes of dynamo-generated flows.

Although we have considered only 2-D strain fields, it is most likely that a similar mechanism of the dynamo saturation via generation of localized large-scale vortex structures exists in 3-D too. Naturally, to be localized such vortices must have shapes of closed loops. Thus, instead of a 2-D vortex quadrupole, two oppositely oriented vortex rings (mirror symmetric with respect to the principal plane of the strain) will be observed.

ACKNOWLEDGMENTS

This work has been performed using the computing facilities provided by the program “Simulations Interactives et Visualisation en Astronomie et Mécanique (SIVAM)” at OCA. Grant from EC (FMRX-CT98-0175) is gratefully acknowledged. The research at the Weizmann Institute has been also supported by the Israeli Science, the Mitchell Research fund and Minerva Foundation, Germany. G.F. is grateful to S. Cowley, A. Fouxon, and J. Maron for useful discussions.

[1] H. K. Moffat, *Magnetic Field Generation in Electrically Conducting Fluids* (Cambridge University Press, Cambridge, England, 1978).

[2] S. Childress and A. Gilbert, *Stretch, Twist, Fold: The Fast Dynamo* (Springer-Verlag, Berlin, 1995).

[3] S. Vainshtein and F. Cattaneo, *Astrophys. J.* **393**, 165 (1992).

[4] R.M. Kulsrud and S.W. Anderson, *Astrophys. J.* **396**, 606 (1992).

[5] Ya.B. Zeldovich, A.A. Ruzmaikin, S.A. Molchanov, and D.D. Sokolov, *J. Fluid Mech.* **144**, 1 (1984).

[6] A. Gruzinov, S. Cowley, and R. Sudan, *Phys. Rev. Lett.* **77**, 4342 (1996).

[7] M. Chertkov, G. Falkovich, I. Kolokolov, and M. Vergassola, *Phys. Rev. Lett.* **83**, 4065 (1999).

[8] S. Kida, S. Yanase, and J. Mizushima, *Phys. Fluids A* **3**, 457 (1991).

[9] B. Galanti, A. Pouquet, and P.L. Sulem, “Influence of the period of an abc flow on its dynamo action,” in *Theory of solar and planetary dynamos* (Cambridge University Press, Cambridge, England, 1993), p. 99.

[10] E. Zienicke, H. Politano, and A. Pouquet, *Phys. Rev. Lett.* **81**, 4640 (1998).

[11] A. Vasilis, Ph.D. thesis, University of Copenhagen, 2000 (unpublished).

[12] C. Nore, M.E. Brachet, H. Politano, and A. Pouquet, *Phys. Plasmas* **4**, 1 (1997).

[13] N. Seehafer, F. Feudel, and O. Schmidtmann, *Astron. Astrophys.* **314**, 693 (1996).

[14] F. Cattaneo, D.W. Hughes, and E.-J. Kim, *Phys. Rev. Lett.* **76**, 2057 (1996).

[15] M. Meneguzzi, U. Frisch, and A. Pouquet, *Phys. Rev. Lett.* **47**, 1060 (1981).

- [16] H.K. Moffatt, *J. Fluid Mech.* **17**, 225 (1968).
- [17] C. Heiles, A. A. Goodman, C. F. Mc Kee, and E. G. Zweibel, in *Protostars and Planets III*, edited by E. H. Levy, J. I. Lunine, M. Guerrieri, and M. S. Matthews (University of Arizona Press, Tucson, 1993), p. 279.
- [18] S.V. Nazarenko, N.K.-R. Kevlahan, and B. Dubrulle, *J. Fluid Mech.* **390**, 325 (1999).
- [19] S.V. Nazarenko, N.K.-R. Kevlahan, and B. Dubrulle, *Physica D* **139**, 158 (2000).